Threshold Collision-induced Dissociation of Hydrated Cadmium (II): Experimental and Theoretical Investigation of the Binding Energies for $Cd^{2+}(H_2O)_n$ Complexes (n = 4 – 11)

Theresa E. Cooper and P. B. Armentrout*

Department of Chemistry, University of Utah, 315 S. 1400 E. Rm 2020, Salt Lake City, UT 84112

Abstract

The first experimentally determined hydration energies of $Cd^{2+}(H_2O)_n$ complexes, n = 4 - 11, are measured using threshold collision-induced dissociation in a guided-ion-beam tandem mass spectrometer coupled with an electrospray-ionization source. Kinetic-energy-dependent cross-sections are obtained and analyzed to yield 0 K thresholds for losing one water ligand. The threshold measurements are converted to 298 K values to give the hydration enthalpies and free energies for sequentially losing one water. Trends in these values and calculations at the MP2(full)/SD/6-311+G(2d,2p)//B3LYP/SD/6-311+G(d,p) level are consistent with the inner-solvent shell of Cd^{2+} being six waters.

Introduction

The hydration of Cd^{2+} is especially interesting because cadmium is highly toxic and environmentally hazardous. Cadmium is particularly dangerous to human health because it is a known carcinogen, nonbiodegradable, and can replace zinc in many biological systems resulting in deactivation of important proteins or enzymes [1]. Cadmium is one of only three metals classified as a priority pollutant by the United States Environmental Protection Agency and is quickly infiltrating aqueous systems. Indeed, emissions of cadmium into the environment are 18 times higher than naturally occurring rates, as cadmium is a major component in rechargeable batteries, electroplating wastewater, and other anthropogenic activities [2,3].

Cadmium coordination behavior has previously been investigated using solid state X-ray structures [1], Raman spectroscopy on aqueous $Cd(ClO_4)_2$ [4], and X-ray absorption fine structure and large angle X-ray scattering studies of the ion in aqueous media [5]. Studies utilizing quantum chemical calculations and molecular dynamics simulations have also been performed [4,6-10]. Most of these studies reported a coordination number for Cd^{2+} of six, forming an octahedral inner shell, although theoretical work of Chillemi et al.[9] suggested that cadmium has an inner solvent shell that varies between hexa- and heptacoordinate, which supported conflicting experimental results of D'Angelo et al. [5].

Despite this work, experimental thermochemistry for the hydration of cadmium cations is presently unknown. To address this lack of thermochemical information, here we examine the dissociation behavior of $Cd^{2+}(H_2O)_n$ complexes, where $n = 4 - 11$. In all cases, the dominant process observed is reaction (1),

$$Cd^{2+}(H_2O)_n \rightarrow Cd^{2+}(H_2O)_{n-1} + H_2O \qquad (1)$$

followed by sequential loss of additional water molecules, although particular sized complexes also undergo a charge separation process, reaction (2).

$$Cd^{2+}(H_2O)_n \rightarrow CdOH^{+}(H_2O)_m + H^{+}(H_2O)_{n-m-1} \qquad (2)$$

Analysis of the kinetic energy dependence of these reactions provides the first experimental determinations of the hydration energies of cadmium cation-water complexes. In related work,

our laboratory has examined the structures and energies of $Zn^{2+}(H_2O)_n$ (also group 12) experimentally and computationally and found that complexes having inner solvent shells of four, five, and six water molecules have similar energies [11,12]. We also determined that the ground state structure and coordination number is highly dependent on the level of theory used and that the MP2(full)//B3LYP level of theory appeared to give the best agreement between experiment and theory. For this reason, in the present paper, we analyze the $Cd^{2+}(H_2O)_n$ data utilizing MP2(full)//B3LYP predicted ground state structures.

Experimental and Theoretical Section

Experimental Procedures

Cross sections for the collision-induced dissociation (CID) of $Cd^{2+}(H_2O)_n$ complexes are measured using a guided ion beam tandem mass spectrometer (GIBMS), which has been described in detail previously [13,14]. Hydrated cadmium dications are generated from 10^{-4} M $Cd(NO_3)_2$ in water using an electrospray ionization (ESI) source [15] comprising a stainless steel electrospray needle, a heated capillary, an 88 plate ion funnel [16], and a hexapole ion guide where the ions undergo sufficient thermalizing collisions to bring them to a Maxwell-Boltzmann distribution at 300 K, as shown previously [15,17-19].

$Cd^{2+}(H_2O)_n$ ions are extracted from the source and mass selected using a magnetic momentum analyzer. Ions are then decelerated to well-defined kinetic energies relative to the ion source, V_{lab}, and focused into a radio frequency (rf) octopole ion guide, trapping the ions radially [20]. A collision gas cell surrounds part of the octopole and contains xenon [21,22], which is introduced to the collision cell at pressures varying between 0.05 and 0.20 mTorr. After collision, reactant and product ions drift to the end of the octopole guide, where they are focused, mass analyzed with a quadrupole mass filter, and detected utilizing a Daly detector [23].

Ion intensities are converted to absolute cross sections with an uncertainty of ±20%, as described previously [13]. In addition, the acceleration voltage applied to the ions in the collision cell, V_{Lab}, is converted to the relative kinetic energy in the center-of-mass (CM) frame

using $E_{CM} = 2\ V_{Lab}\ m/(m + M)$, where $m + M$ are the masses of Xe and the ionic reactant, respectively, and the factor of two accounts for the charge on the reactant complexes. The absolute energy zero and kinetic-energy distribution of the reactant ions are determined using a retarding potential technique [13]. The full width at half maximum (FWHM) for the V_{Lab} distribution ranges from 0.08 – 0.13 eV. The absolute uncertainty in V_{Lab} is 0.05 eV. All energies below are reported in the CM frame.

Threshold Modeling

To extract accurate thermochemical results from analysis of the kinetic-energy dependent cross sections, several factors must be considered. Experiments were performed at three different pressures of Xe (~ 0.05, 0.10, and 0.20 mTorr) and the resulting cross sections extrapolated to zero pressure to ensure single collision conditions [24,25]. This zero pressure cross section is modeled using the empirical threshold model, Eq. (3).

$$\sigma(E) = \sigma_0 \Sigma\ g_i\ (E + E_i - E_0)^N / E \qquad (3)$$

Here, σ_0 is an energy independent scaling factor, E is the relative translational energy of the reactants, E_0 is the reaction threshold at 0 K, and N is an adjustable fitting parameter that describes the energy deposition upon collision [14]. The summation is over the rovibrational states of the reactants having excitation energies E_i and populations g_i, where $\Sigma g_i = 1$. The number of rovibrational states is directly counted using the Beyer-Swinehart Stein-Rabinovitch algorithm [26-29] and a Maxwell-Boltzmann distribution at 300 K is used to describe the populations g_i. Before comparison with the data, the model is also convoluted over the kinetic energy distributions of the reactants [13].

As the $Cd^{2+}(H_2O)_n$ ions become larger, their dissociation lifetime near threshold can become comparable to the experimental time of flight, $\tau \approx 5 \times 10^{-4}$ s. This behavior can give rise to a kinetic shift that is accounted for by incorporating Rice-Ramsperger-Kassel-Marcus (RRKM) theory [29,30] into Eq. (3), as discussed in detail elsewhere [31-33], and shown in Eq. (4).

UU IR Author Manuscript

$$\sigma(E) = (N\sigma_0/E)\sum g_i \int_{E_0-E_i}^{E} \left[1 - e^{-k(\varepsilon+E_i)\tau}\right](E-\varepsilon)^{N-1} d\varepsilon \quad (4)$$

Here ε is the energy transferred into the reactant ion by the collision. When the unimolecular rate constant is faster than the experimental time scale, Eq. (4) reduces to Eq. (3). The RRKM unimolecular rate constant, $k(\varepsilon + E_i) = k(E^*)$, is given by Eq. (5),

$$k(E^*) = sN^{\dagger}_{vr}(E^* - E_0) / h\rho_{vr}(E^*) \quad (5)$$

where s is the reaction degeneracy, $N^{\dagger}_{vr}(E^* - E_0)$ is the sum of the ro-vibrational states of the transition state (TS), and $\rho_{vr}(E^*)$ is the density of ro-vibrational states for the energized molecule (EM). Vibrational frequencies and rotational constants for the EM and TS are taken from the calculations discussed below. For water loss channels, the TS is loose because the bond cleavage is heterolytic with all the charge remaining on the complex containing the cadmium ion [34]. The TS for water loss is treated at the phase space limit (PSL) in which the TS is product-like and the transitional modes are treated as rotors [33].

Analysis of the data involves using Eqs. (3) or (4) to reproduce the data over extended energy and magnitude ranges, using a least-squares criterion for optimizing the fitting parameters, σ_0, E_0, and N. The uncertainties in these parameters include variations associated with modeling several independent experimental cross sections, scaling the theoretical vibrational frequencies by ±10%, varying the N value by ±0.1, scaling the experimental time of flight up and down by a factor of two, and the uncertainty in the absolute energy scale.

Computational Details

Calculations were performed using the *Gaussian03* package [35], using structures found previously[11] for $Zn^{2+}(H_2O)_n$ complexes as starting geometries for the $Cd^{2+}(H_2O)_n$ complexes. Geometry optimizations were performed at the B3LYP [36,37] level of theory with a 6-311+G(d,p) basis set on the waters and the small core (28 electron) Stuttgart-Dresden (SD) effective core potential (ECP) on Cd^{2+}, as obtained from the EMSL basis set exchange [38]. Vibrational frequencies and rotational constants were also calculated at this level of theory.

UU IR Author Manuscript

Frequencies were scaled by 0.989 [39] before being used in the RRKM analysis described above, as well to calculate zero point energy (ZPE) and thermal corrections. Single point energies (SPEs) were calculated at the MP2(full)[40]/SD/6-311+G(2d,2p) level. Basis set superposition error (BSSE) corrections were calculated for dissociation of the lowest energy structures in the full counterpoise (cp) limit [41,42].

Results and Discussion

Cross sections for CID

Experimental CID cross sections for $Cd^{2+}(H_2O)_n$, where n = 4 – 11, were acquired and representative data for n = 5 and 8 are shown in Figure 1. In all cases, the dominant process is the loss of a water molecule, reaction (1). This is followed by loss of additional water molecules as the kinetic energy increases, forming the smallest observable $Cd^{2+}(H_2O)_2$ complex. Products of reaction (2) are also observed, $CdOH^+(H_2O)_m$ and $H^+(H_2O)_{n-m-1}$, and are shown as the total "charge separation" cross section. There are several independent charge separation processes that complicate the dissociation of $Cd^{2+}(H_2O)_5$, $Cd^{2+}(H_2O)_4$, and possibly $Cd^{2+}(H_2O)_3$, and these reactions will be examined in a future publication. For the present work, it is important to note that the $Cd^{2+}(H_2O)_4$ complex undergoes reaction (2), with m = 2, at a lower energy than loss of a water molecule in reaction (1). As demonstrated previously [12], in such a case, it is necessary to include the competition between these two dissociation channels when analyzing the data to extract an accurate hydration energy.

Theoretical geometries of ground state cadmium water clusters

In the geometries for n = 1 – 6, all water ligands bind directly to the cadmium ion, in agreement with previous works [9,10], and are comparable to structures reported for $Zn^{2+}(H_2O)_n$ and $Ca^{2+}(H_2O)_n$ [11,17]. Not surprisingly, the cadmium complexes have longer metal oxide bond distances than their zinc analogues by 0.20 – 0.23 Å because the cadmium ion radius is larger by 0.21 Å (0.99 Å for Cd^{2+} versus 0.78 Å for Zn^{2+}), but have shorter metal oxide bonds

UU IR Author Manuscript

than the analogous calcium complexes by 0.08 – 0.18 Å because of the larger ion radius of Ca^{2+} (1.05 Å) [43]. The $Cd^{2+}(H_2O)_n$, where n = 1 – 6, complexes have C_{2v}, D_{2d}, D_3, S_4, C_{2v}, and T_h symmetries, respectively. As also found previously [10], the $Cd^{2+}(H_2O)_3$ complex is slightly more symmetric than $Zn^{2+}(H_2O)_3$, which only has C_2 symmetry.

For n = 7, the ground state (GS) structure is the $Cd^{2+}(H_2O)_6(H_2O)_1$ or (6,1)_AA complex with no symmetry (C_1), which has an octahedral inner solvent shell of six and the seventh water begins a second shell by forming two hydrogen acceptor bonds (denoted "AA"), Figure 2c. Pye et al. [10] report a slightly different (6,1)_AA complex having C_2 symmetry (such that there are fewer hydrogen bonds between water molecules in the inner shell), which we find to be higher in energy by 3 kJ/mol at 0 K, after including ZPE corrections (3 kJ/mol for $\Delta\Delta G_{298}$, after thermal corrections to 298 K) at the present MP2(full) level. Chillemi et al. [9] reported a (7,0) GS with C_2 symmetry using a Hartree Fock (HF) level of theory with the LANL2DZ ECP on Cd^{2+} and a cc-pVTZ basis set on the waters. However, we find that (7,0), Figure 2d, is higher than the (6,1)_AA complex by 23 kJ/mol at 0 K (19 kJ/mol for $\Delta\Delta G_{298}$). This is in accord with the theoretical and experimental results from Pye and co-workers [10], who found that (7,0) is about 20 kJ/mol higher in energy than their (6,1)_AA complex at both the HF and MP2 levels using a number of different basis sets and ECPs. They also found no evidence of a heptacoordinate structure using Raman spectroscopy. Structures having an inner solvent shell of five or four waters were also investigated, Figure 2. Compared to (6,1)_AA, the square pyramidal inner solvent shell of (5,2)_2A_bA_b (the "b" denotes the water hydrogen bonds to the base of the square pyramid) is 9 kJ/mol higher (14 kJ/mol for $\Delta\Delta G_{298}$). The (4,3)_2AA,A complex is 37 kJ/mol ($\Delta\Delta G_{298}$ = 39 kJ/mol) higher in energy, forming a pseudo-tetrahedral inner shell with two second shell waters forming two hydrogen bonds and the third forming only a single hydrogen bond to the inner shell (denoted "A"). The MP2(full) level favors a six inner solvent shell over inner shells of four or five by about 10 – 60 kJ/mol depending on the complex size. For this reason, we no longer discuss inner solvent shells besides six here, although preliminary results suggest

UU IR Author Manuscript

that DFT levels of theory predict the GS structures for $n \geq 6$ may have inner solvent shells of four or five waters.

For larger complexes, many structures have similar H-bonding in the second solvation shell. Accordingly our nomenclature includes terms "D" or "DD" to describe an inner shell water that donates to a second shell water with one or two H-bonds, respectively. For $n = 8$, the (6,2)_4D_2AA in which two pairs of inner shell waters form two H-bonds with the outer shell waters, is both the 0 K and 298 K GS complex, in agreement with previous work [17] on $Ca^{2+}(H_2O)_n$. For $n = 9$, two complexes are close in energy, the (6,3)_6D_3AA and (6,3)_4D,DD_3AA, which are analogous to structures in the $Ca^{2+}(H_2O)_n$ study. At the MP2(full) level, the former is the 0 K GS, but is 4 kJ/mol higher in free energy at 298 K whereas the latter is 2 kJ/mol higher at 0 K enthalpy. Similar to the (6,4) complexes reported for $Zn^{2+}(H_2O)_{10}$ [11], the (6,4)_4D,2DD_4AA is the GS complex at both 0 K and 298 K. The 298 K GS structure for $n = 11$ is the (6,5)_4AA,A complex, however, the (6,5)_AA,AAD,AA_p complex is lower at 0 K by 4 kJ/mol (8 kJ/mol higher for $\Delta\Delta G_{298}$), Figure 3. In the latter complex, two of the outer shell waters H-bond to one another, thereby forming a "pseudo third shell" and a ring-like series of H-bonds denoted by the AAD,AA_p naming scheme.

Thermochemical Results

Using Eqs. (3) and (4), the total cross sections for the primary water loss of $Cd^{2+}(H_2O)_n$, where $n = 4 - 11$, were modeled. Table 1 summarizes the average parameters obtained and a representative model of $Cd^{2+}(H_2O)_6$ using Eq. (4) is shown in Figure 4. In modeling reaction (1), the reactant isomer is assumed to be the 298 K GS (as this species should have the dominant population in a thermally equilibrated source) and the product isomer is the 0 K GS (as our threshold analysis is dominated by the lowest 0 K enthalpy species) [11]. For the remainder of this paper, the nomenclature of the GS structures is abbreviated as (x,y), where x is the number of waters in the first solvent shell and y is the number of waters in the second solvent shell. For instances when the 298 K GS differs from the 0 K GS, the full name of the 298 K GS is given.

UU IR Author Manuscript

The difference between modeling with (Eq. (4)) and without (Eq. (3)) RRKM is the kinetic shift, which is appreciable for most complexes, and increases from 0.18 eV at n = 4 to 0.68 eV at n = 11. As discussed above, the n = 4 water loss is complicated by reaction (2) such that this competition should be accounted for in order to obtain an accurate threshold measurement. This analysis requires details of the TS for reaction (2) as well as including statistical RRKM theory for each competing reaction channel, which is beyond the scope of the present work. In our previous zinc hydration study [12], we found a competitive shift of 0.08 eV (8 kJ/mol) for the analogous dissociation. For the purposes of the present investigation, our best measure of the n = 4 threshold includes this approximate correction for competition.

The reaction thresholds decrease as the complex size increases. This decrease is relatively small between the complexes in the range of n = 7 – 11, whereas large decreases are seen between n = 4 – 7. The large decrease from n = 6 to 7 suggests that the sixth water is more tightly bound to the complex, implying an inner solvent shell of six. Another large threshold difference is seen between n = 4 and 5. The high threshold for $Cd^{2+}(H_2O)_4$ can be understood by the 18 electron rule, which is fulfilled at this complex size.

Comparison to Theory

Figure 5 is a direct comparison of experimental and theoretical 0 K bond dissociation energies (BDEs) including zero point energy and cp corrections, as listed in Table 2. The theoretical BDEs show similar qualitative trends to the experimental values. Namely, BDEs in the range of n = 7 – 11 decrease slowly, whereas there is a large decrease from n = 6 to 7 and another large decrease from n = 4 to 5, as discussed above. Our experimental values for n = 6 – 11 are slightly lower than the MP2(full)/SD/6-311+G(2d,2p) theoretical calculations, but each are within 10 kJ/mol, about twice our experimental uncertainty. For n = 4, the threshold value of 147.6 kJ/mol agrees within ~3 kJ/mol of the cp-corrected SD result, reaffirming the need to include the competitive shift discussed above.

UU IR Author Manuscript

Electronic binding energies have also been reported in the literature for $n = 4 - 7$, but use a smaller basis set than used here and were not corrected for zero point energies or BSSE [10,44]. These values are given in Table 2 after correcting by the zero point energies calculated here. For $n = 4 - 6$, the literature values tend to overestimate the 0 K hydration energies at the MP2 level by up to 10 kJ/mol compared to the present MP2(full) results without cp correction. However, the $n = 7$ literature dissociation value is lower in energy by 11 kJ/mol, where the structural and energetic differences discussed above for the two (6,1)_AA complexes partially account for this difference.

Conversion from 0 K to 298 K

Using the vibrational frequencies and rotational constants of the cadmium water clusters calculated during the geometry optimization at the B3LYP/SD/6-311+G(d,p) level of theory discussed above, a rigid rotor/harmonic oscillator approximation was applied to convert the 0 K bond energies to 298 K hydration enthalpies and free energies, ΔH_{298} and ΔG_{298}, respectively, in Table 3. The uncertainties in these conversions are found by scaling the vibrational frequencies up and down by 10%.

Like the hydration energies, the free energies of hydration decrease as the size of the $Cd^{2+}(H_2O)_n$ increases. The $\Delta\Delta G_{298}$ values also decease as the complexes increase in size. The entropies of dissociation, $T\Delta S_{298}$, remain relatively constant as there are no major solvent shell rearrangements between these structures.

Conclusions and Future Work

The kinetic-energy dependent cross sections for collision-induced dissociation of $Cd^{2+}(H_2O)_n$, where $n = 4 - 11$, have been determined using guided ion beam mass spectrometry. The results presented here are the first reported experimental bond energies of the hydrated cadmium ion. For all values of n studied, the dominant process is the sequential loss of a single water molecule from the $Cd^{2+}(H_2O)_n$ species. A charge separation reaction occurs in competition

UU IR Author Manuscript

with the loss of a water ligand at the n = 5, 4, and possibly 3 complexes, and is energetically favored over water loss at the n = 4 complex. Including this competition at the n = 4 complex is necessary for obtaining the most accurate energetic information, and will be performed explicitlyfor this system and described in detail in a future publication.

Our theoretical work also represents the first structures and energetics determined for $Cd^{2+}(H_2O)_n$, where n = 8 – 11. MP2(full)/SD/6-311+G(2d,2p) results find that the GS structures of Cd^{2+} are hexacoordinate with all six waters bound directly to the cadmium ion, in agreement with previous work [1,4,6-10]. The results after cp correction give good agreement with our experimental values with an overall mean absolute deviation (MAD) of 6.5 kJ/mol (16.5 kJ/mol without cp correction). Continued investigation using other ECPs and levels of theory is underway and will include consideration of multiple conformers for n = 5 – 11. Previous work on zinc hydration [11] demonstrated that the experimental values obtained for the water-loss dissociation energies were slightly influenced by the ground state structure chosen for data analysis, where this dependence is a result of ambiguous theoretical results instead of experimental error. Because of this dependence, comprehensive data analysis will take place using all predicted low energy isomers for $Cd^{2+}(H_2O)_n$. Although not definitive at this point, previous comparisons between theory and experiment suggest that the structural predictions of MP2(full) theory are more reliable for this type of complex [11], indicating that most cadmium complexes studied here are likely to have six-coordinate inner hydration shells. Such conclusions are tempered by the observation that because these complexes have many floppy motions, both zero point and thermal corrections utilizing scaled harmonic frequencies lead only to an approximation of the true 0 and 298 K energies.

Acknowledgement

This work is supported by the National Science Foundation, Grant No. CHE-0748790. In addition, we thank the Center for High Performance Computing at the University of Utah for the generous allocation of computer time.

UU IR Author Manuscript

Table1

Optimized parameters of Eqs. (3) and (4) from analysis of CID cross sections [a]

Reactant	Product	σ_0 [b]	N [b]	E_0 (eV)[c]	E_0 (PSL, eV) [b]
(4,0)	(3,0)	52 (3)	0.6 (0.1)	1.79 (0.06)	1.61 (0.05)[d]
(5,0)	(4,0)	70 (4)	0.8 (0.1)	1.24 (0.07)	1.11 (0.05)
(6,0)	(5,0)	64 (4)	0.9 (0.1)	1.05 (0.09)	0.90 (0.05)
(6,1)	(6,0)	80 (4)	0.8 (0.1)	0.94 (0.07)	0.70 (0.05)
(6,2)	(6,1)	96 (5)	0.8 (0.1)	0.97 (0.05)	0.66 (0.06)
(6,3)[e]	(6,2)	109 (2)	0.8 (0.1)	0.97 (0.04)	0.61 (0.05)
(6,4)	(6,3)	95 (6)	0.9 (0.1)	0.98 (0.07)	0.49 (0.05)
(6,5)[f]	(6,4)	59 (4)	1.1 (0.1)	1.11 (0.1)	0.43 (0.05)

[a] Uncertainties in parentheses.

[b] Parameters from modeling with Eq. (4), where RRKM analysis is used to account for lifetime effects.

[c] Thresholds from modeling with Eq. (3), where no RRKM analysis is used.

[d] 1.53 ± 0.05 eV after a competitive shift of 0.08 eV is applied.

[e] (6,3)_4D,DD_3AA isomer.

[f] (6,5)_4AA,A isomer.

UU IR Author Manuscript

Table 2

Comparison of experimental 0 K bond energies (kJ/mol) to theoretical values.

n	Reactant	Product	Experiment [a]	MP2(full)// B3LYP [b]	MP2/ 6-31+G* [c]
4	(4,0)	(3,0)	147.6 (4.8)	144.4 / 158.6	168.0 (177.5)
5	(5,0)	(4,0)	107.1 (4.8)	106.7 / 121.2	128.3 (137.8)
6	(6,0)	(5,0)	86.8 (4.8)	97.3 / 113.7	120.5 (126.5)
7	(6,1)	(6,0)	67.5 (4.8)	71.3 / 80.5	69.7 (75.7)
8	(6,2)	(6,1)	63.7 (5.8)	73.5 / 82.3	
9	(6,3)[d]	(6,2)	58.9 (4.8)	67.7 / 76.4	
10	(6,4)	(6,3)	47.3 (4.8)	55.4 / 64.0	
11	(6,5)[e]	(6,4)	41.5 (4.8)	48.9 / 55.6	
MAD				6.5 / 16.5	19.4 (27.1)

[a] Values from Table 1 including the correction for competition at $n = 4$.

[b] MP2(full)/SD/6-311+G(2d,2p)//B3LYP/SD/6-311+G(d,p) level. ZPE corrected. Values listed with / without cp correction.

[c] Values from Pye et al. [10] after ZPE corrections using vibrational frequencies calculated here with the original values in parentheses [44].

[d] (6,3)_4D,DD_3AA isomer.

[e] (6,5)_4AA, A isomer.

UU IR Author Manuscript

Table 3

Conversion of 0 K thresholds to 298 K enthalpies and free energies for water loss from $Cd^{2+}(H_2O)_n$. All values in kJ/mol with uncertainties in parentheses.

n	Dissociation	ΔH_0[a]	$\Delta H_{298} - \Delta H_0$[b]	ΔH_{298}	$T\Delta S_{298}$[b]	ΔG_{298}
4	(4,0) → (3,0)	147.6 (4.8)	1.3 (0.5)	148.9 (4.8)	33.5 (1.3)	115.4 (5.0)
5	(5,0) → (4,0)	107.1 (4.8)	2.4 (0.6)	109.5 (4.8)	43.4 (1.4)	66.1 (5.0)
6	(6,0)→ (5,0)	86.8 (4.8)	1.6 (0.5)	88.4 (4.8)	42.3 (1.4)	46.1 (5.0)
7	(6,1) → (6,0)	67.5 (4.8)	3.4 (0.4)	70.9 (4.8)	35.9 (1.0)	35.0 (4.9)
8	(6,2) → (6,1)	63.7 (5.8)	4.1 (0.4)	67.8 (5.8)	43.5 (1.0)	24.3 (5.9)
9	(6,3)[c] → (6,2)	58.9 (4.8)	4.1 (0.4)	63.0 (4.8)	42.5 (1.0)	20.5 (4.9)
10	(6,4) → (6,3)	47.3 (4.8)	1.4 (0.3)	48.7 (4.8)	31.3 (1.2)	17.4 (4.9)
11	(6,5)[d] → (6,4)	41.5 (4.8)	1.5 (0.4)	43.0 (4.8)	32.5 (1.3)	10.5 (5.0)

[a] Experimental values from Table 2.

[b] Values calculated from the vibrations and rotations calculated at the B3LYP/SD/6-311+G(d,p) level. Uncertainties found by scaling the frequencies up and down by 10%.

[c] (6,3)_4D,DD_3AA isomer.

[d](6,5)_4AA,A isomer.

References

[1] D.T. Richens, The Chemistry of Aqua Ions, John Wiley and Sons, Inc, New York, 1997.

[2] W. Salomons, U. Förstner, P. Mader, Heavy metals : problems and solutions, Springer-Verlag, Berlin ; New York, 1995.

[3] J.E. Fergusson, The heavy elements : chemistry, environmental impact, and health effects, Pergamon Press, Oxford ; New York, 1990.

[4] W.W. Rudolph, C.C. Pye, J. Phys. Chem. B 102 (1998) 3564.

[5] P. D'Angelo, G. Chillemi, V. Barone, G. Mancini, N. Sanna, I. Persson, J. Phys. Chem. B 109 (2005) 9178.

[6] E.P.F. Lee, P. Soldan, T.G. Wright, J. Phys. Chem. A 105 (2001) 8510.

[7] T.S. Hofer, H.T. Tran, C.F. Schwenk, B.M. Rode, J. Comput. Chem. 25 (2004) 211.

[8] C. Kritayakornupong, K. Plankensteiner, B.M. Rode, J. Phys. Chem. A 107 (2003) 10330.

[9] G. Chillemi, V. Barone, P. D'Angelo, G. Mancini, I. Persson, N. Sanna, J.Phys. Chem. B 109 (2005) 9186.

[10] C.C. Pye, M.R. Tomney, W.W. Rudolph, Can. J. Anal. Sci. Spect. 51 (2006) 140.

[11] T.E. Cooper, D. Carl, P.B. Armentrout, J. Phys. Chem. A 113 (2009) 13727. .

[12] T.E. Cooper, P.B. Armentrout, J. Phys. Chem. A 113 (2009) 13742.

[13] K.M. Ervin, P.B. Armentrout, J. Chem. Phys. 83 (1985) 166.

[14] F. Muntean, P.B. Armentrout, J. Chem. Phys. 115 (2001) 1213.

[15] R.M. Moision, P.B. Armentrout, J. Am. Soc. Mass Spectrom. 18 (2007) 1124.

[16] T. Kim, H.R. Udseth, R.D. Smith, Anal. Chem. 72 (2000) 5014.

[17] D.R. Carl, R.M. Moision, P.B. Armentrout, Int. J. Mass Spectrom. 265 (2007) 308.

[18] A.L. Heaton, R.M. Moision, P.B. Armentrout, J. Phys. Chem. A 112 (2008) 3319.

[19] A.L. Heaton, S.J. Ye, P.B. Armentrout, J. Phys. Chem. A 112 (2008) 3328.

[20] D. Gerlich, Adv. Chem. Phys. 82 (1992) 1.

[21] N.F. Dalleska, K. Honma, L.S. Sunderlin, P.B. Armentrout, J. Am. Chem. Soc. 116 (1994) 3519.

[22] N. Aristov, P.B. Armentrout, J. Phys. Chem. 70 (1986) 4111.

UU IR Author Manuscript

[23] N.R. Daly, Rev. Sci. Instrum. 31 (1960) 264.

[24] D.A. Hales, L. Lian, P.B. Armentrout, Int. J. Mass Spectrom. Ion Process. 102 (1990) 269.

[25] R.H. Schultz, K.C. Crellin, P.B. Armentrout, J. Am. Chem. Soc. 113 (1991) 8590.

[26] S.E. Stein, B.S. Rabinovich, Chem. Phys. Lett. 49 (1977) 1883.

[27] T.S. Beyer, D.F. Swinehart, Comm. Assoc. Comput. Mach. 16 (1973) 379.

[28] S.E. Stein, B.S. Rabinovich, J. Chem. Phys. 58 (1973) 2438.

[29] R.G. Gilbert, S.C. Smith, Theory of Unimolecular and Recombination Reactions, Blackwell Scientific, Oxford, 1990.

[30] K.A. Holbrook, M.J. Pilling, S.H. Robertson, Unimolecular Reactions, Wiley, New York, 1996.

[31] S.K. Loh, D.A. Hales, L. Lian, P.B. Armentrout, J. Chem. Phys. 90 (1989) 5466.

[32] F.A. Khan, D.E. Clemmer, R.H. Schultz, P.B. Armentrout, J. Phys. Chem. 97 (1993) 7979.

[33] M.T. Rodgers, K.M. Ervin, P.B. Armentrout, J. Chem. Phys. 106 (1997) 4499.

[34] P.B. Armentrout, J. Simons, J. Am. Chem. Soc. 114 (1992) 8627.

[35] M.J. Frisch, e. al., Gaussian 03, Revision B.02. Gaussian, Inc., Pittsburgh, PA, 2003.

[36] A.D. Becke, J. Chem. Phys. 98 (1993) 5648.

[37] C. Lee, W. Yang, R.G. Parr, Phys. Rev. B 37 (1988) 785.

[38] K.L. Schuchardt, B.T. Didier, T. Elsethagen, L.S. Sun, V. Gurumoorthi, J. Chase, J. Li, T.L. Windus, J. Chem. Inf. Model. 47 (2007) 1045.

[39] C.W. Bauschlicher Jr., H. Partridge, J. Chem. Phys. 103 (1995) 1788.

[40] C. Moller, M.S. Plesset, Phys. Rev. B 46 (1934) 618.

[41] S.F. Boys, R. Bernardi, Mol. Phys. 19 (1970) 553.

[42] F.B. van Duijneveldt, J.G.C. van Duijneveldt, J.H. van Lenthe, Chem. Rev. 94 (1994) 1873.

[43] R.G. Wilson, G.R. Brewer, Ion Beams with Applications to Ion Implantation, Wiley, New York, 1973.

[44] C.C. Pye, personal communication, October 13, 2009.

UU IR Author Manuscript

Figure Captions.

Figure 1. CID cross sections for the sequential water loss (open symbols) and charge separation (lines) processes for $Cd^{2+}W_n$ where W = H_2O for n = 5 and 8 (parts a and b, respectively) colliding with Xe at 0.2 mTorr as a function of energy in the laboratory (upper x-axis) and center of mass (lower x-axis) frames.

Figure 2. Low energy isomers of $Cd^{2+}(H_2O)_7$ calculated at the B3LYP/SD/6-311+G(d,p) level of theory.

Figure 3. Ground state isomers of $Cd^{2+}(H_2O)_{11}$ calculated at the B3LYP/SD/6-311+G(d,p) level of theory. Part a is the 298 K free energy GS and part b is the 0 K GS calculated according to the MP2(full)/SD/6-311+G(2d,2p) level of theory.

Figure 4. Zero pressure extrapolated cross sections for the CID of $Cd^{2+}(H_2O)_6$ with Xe. The solid line shows the best fit to the data using Eq. (4) convoluted over the kinetic and internal energy distributions of the neutral and ion. The dashed line shows the model in the absence of experimental kinetic energy broadening for reactions with an internal energy of 0 K.

Figure 5. Comparison of experimental (solid symbols) and theoretical (open symbols) hydration enthalpies at 0 K. All theoretical results shown are zero point energy and counterpoise corrected. The (6,3) and (6,5) isomers correspond to (6,3)_4D,DD_3AA and (6,5)_4AA,A, respectively.

UU IR Author Manuscript

a)

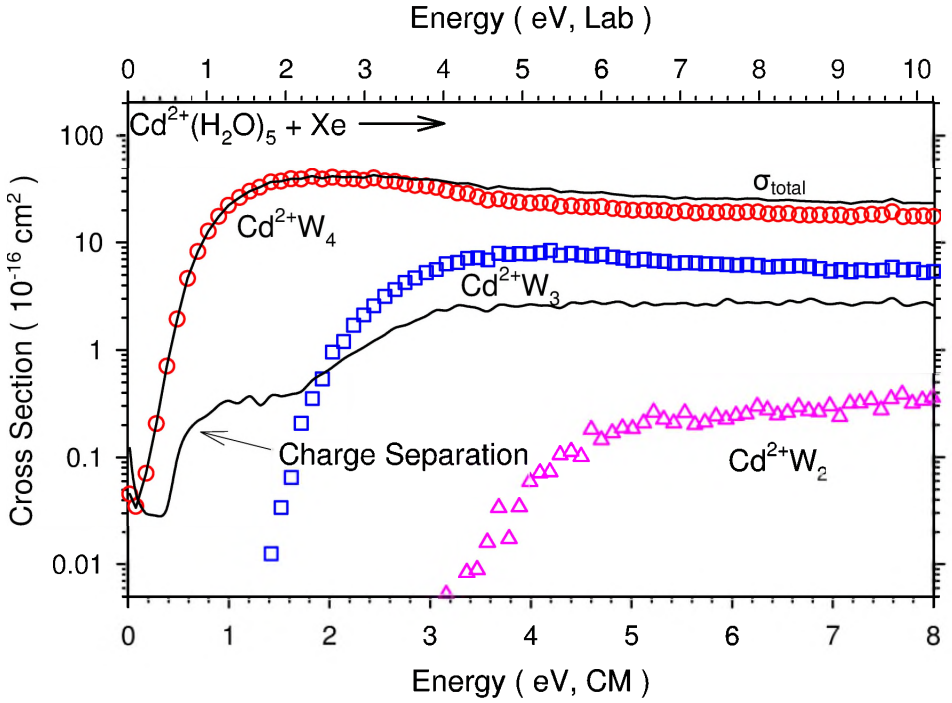

b)

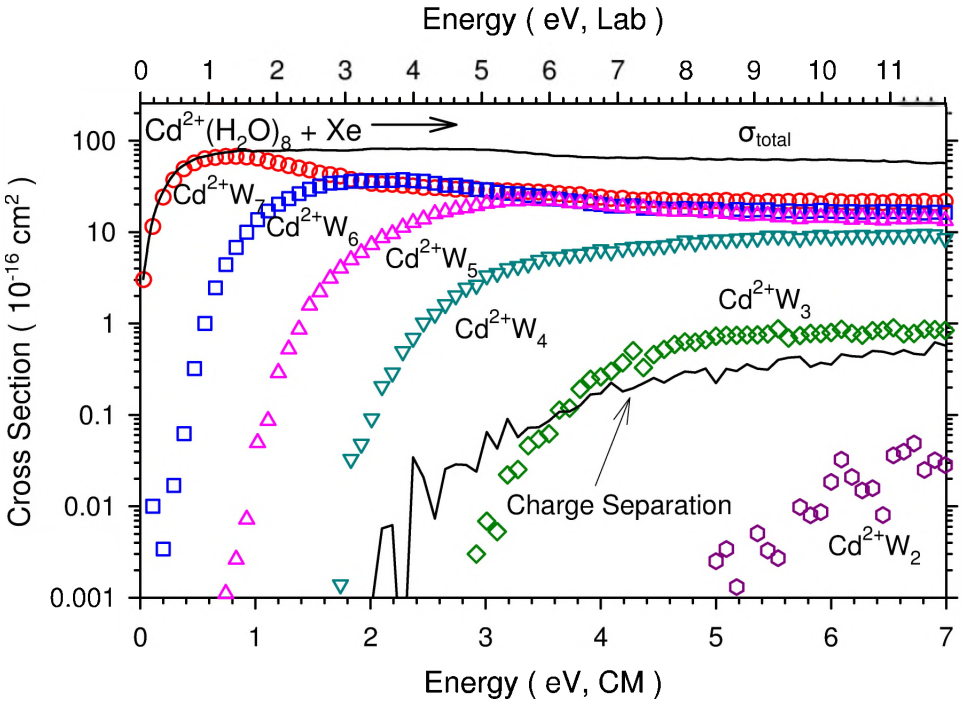

Figure 1

UU IR Author Manuscript

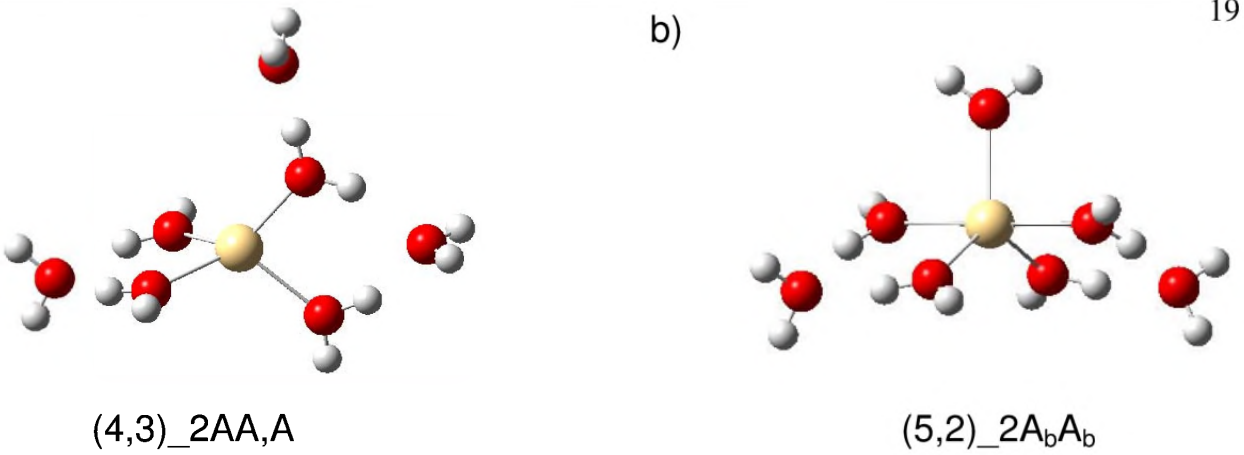

Figure 2

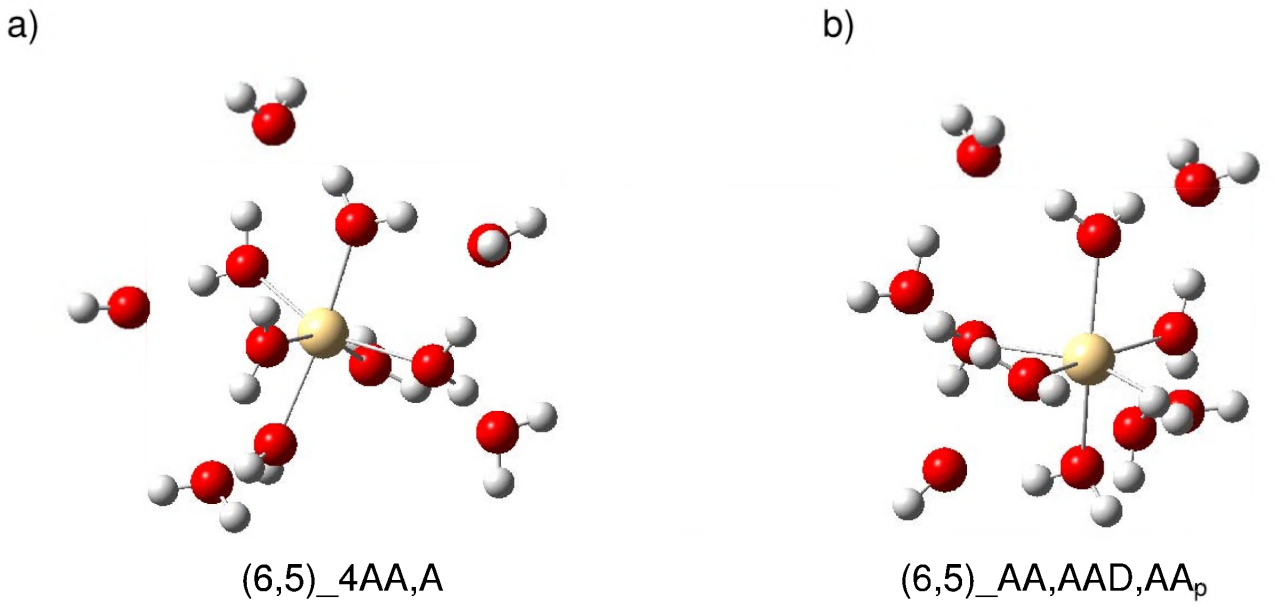

Figure 3

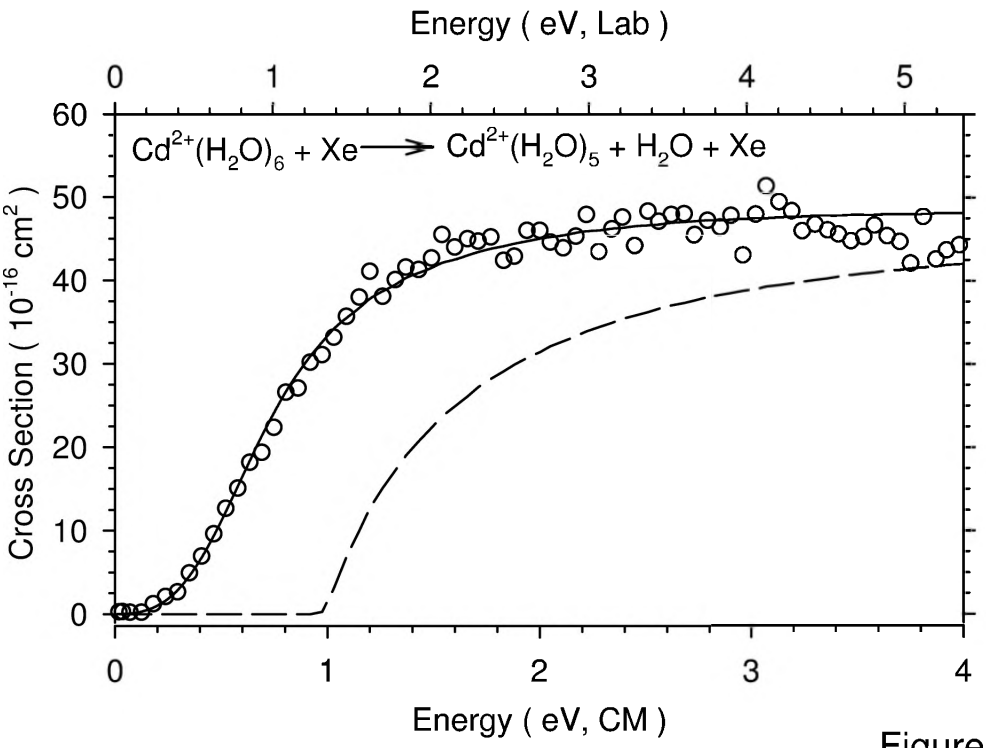

Figure 4

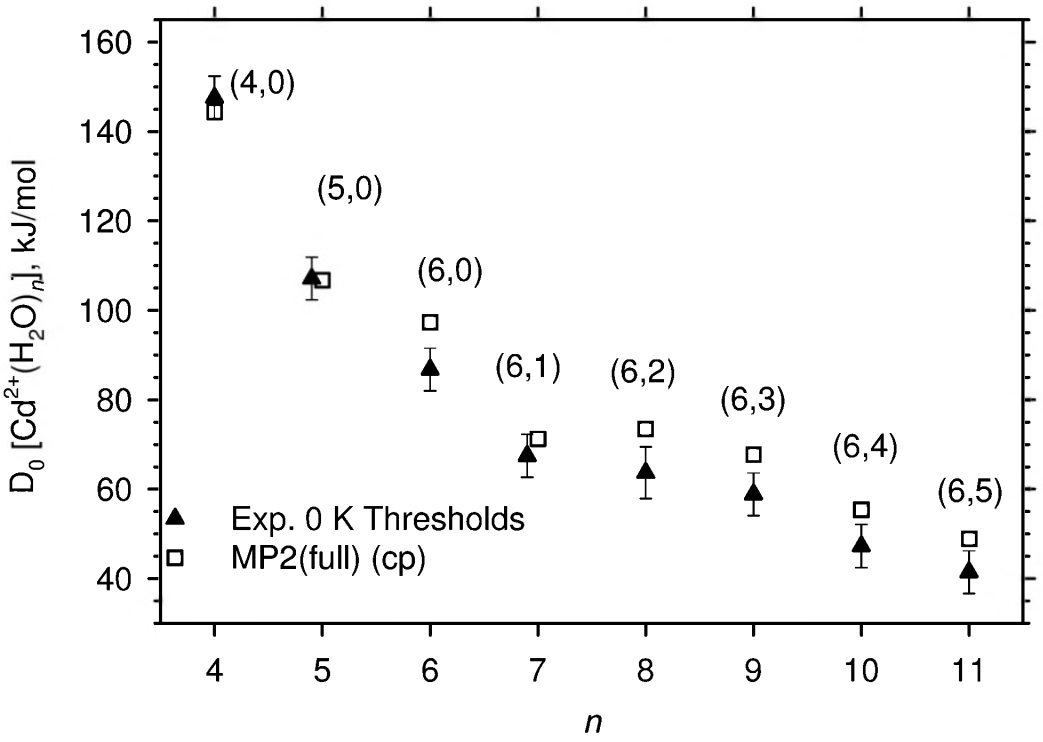

Figure 5